

Structural Analysis and Optimization of a UAV wing

João Francisco Matos Alves Ferreira
Joao.alves.ferreira@tecnico.ulisboa.pt

Instituto Superior Técnico, Universidade de Lisboa, Portugal

November 2018

Abstract

The use of unmanned aerial vehicles, also known as UAVs, are extremely useful on environmental operations such as on the measure of the gases emitted by a boat, in maritime accidents and in forest fires. By being controlled from a distant point, having a reasonable autonomy and agility, those vehicles came to add an efficiency on the results of those operations. It is also a safer procedure where there are no human lives in danger. The composite materials play a key role in the UAVs structure, being its optimization a real need, namely in the wings.

The present study was developed with “UAVision”, doing the structural analysis and topology optimization of the wing of one of their UAVs. The main goal is to implement the optimization multiobjective derivative-free method called “direct multisearch” (DMS), to minimize the maximum deflection and mass of the wing, to improve the autonomy of the vehicle and its flight stability. The DMS solver uses the concept of Pareto dominance to define a list of nondominated points, from which the new iterates are chosen.

A 3D model based on the current wing dimensions (*SolidWorks* model, courtesy of “UAVision”) was built from scratch, using the commercial software *ANSYS Mechanical APDL 18.1*. Assuming stationary flight conditions, was used the *XFLR5* software to obtain the distributed lifting forces to apply on the wing. For the topology optimization was used the *MATLAB R2015a* software (using the DMS).

Was achieved 17 acceptable wing geometries, reaching a maximum decrease of 0.3% of the maximum wing deflection and 8% of the wing mass.

Keywords: UAV, wing, structural analysis, composite materials, DMS, multiobjective optimization

1. Introduction

The Unmanned Aerial Vehicles (UAVs), as it is defined in [1], are “aerial vehicles that do not carry a human operator, use aerodynamic forces to provide vehicle lift, can fly autonomously or be piloted remotely, can be expendable or recoverable, and carry a lethal or nonlethal payload.” They can be powered by several types of engines, such as combustion (the case of this work) and electrical engines. Those type of vehicles are not new in the engineering field. Actually, the first kind of pilotless object was developed in 1918, in a military environment as a type of long-range artillery [2]. As it is commonly seen in the technological evolutionary process, in the case of the UAVs, the wars had a key role: from the WWII to the most recent ones, such as Iraq (2003), Afghanistan (2001) and Kosovo (1999) [1,2].

Besides the military applications, the truth is that UAVs perform an extensive number of civil tasks, namely environmental.

Nowadays, problems such as oil splits and forest fires are a real problem, and the prevention and control of those accidents are extremely important. In that conditions, UAVs are a reliable and safe alternative to accomplish the tasks successfully [3,4].

The present work was made in collaboration with the “UAVision” company. “UAVision” is a Portuguese company, founded by some alumni from “Técnico Lisboa” in 2005. Nowadays they are “experts in development, production and marketing of fixed-wing and multi-rotors” UAVs. They also design and produce some sensors for different applications and other kind of technological innovations like “instrumented buoys for monitoring of the sea and environmental parameters”. Their UAVs have been using in different countries, in military, environmental and civil applications. The big majority of the electronics and structural components of their products are developed and manufactured in their

premises (address: Casais da Arriota, 26 Bonabal 2565-835 Ventosa Portugal) [5].

The component in study is the wing of the UAV showed in Figure 1. The structural analysis was based on the dimensions imposed by the company (*SolidWorks* model, courtesy of “UAVision”), as well as the materials, since it is expected to produce the optimal version of the wing with the resources available. Because of that, it was made a topology optimization, being the external geometry of the wing preserved, Figure 2. The structure is constituted by several ribs, some spars, two winglets and some internal and external holes for the electrical and other structural components.

The main goal of this work is to optimize topologically the wing, using the “direct multisearch” solver (DMS) [6], minimizing the maximum deflection of the wing and its mass value. Since the materials are the available ones in the “UAVision” company (the same already being used), the mass can be reduced manipulating the thickness of the materials and the number of laminas in the carbon-epoxy composite components. Based on that and modifying the positions of the spars, the value of the maximum deflection changes.



Figure 1 - UAV in study [5]

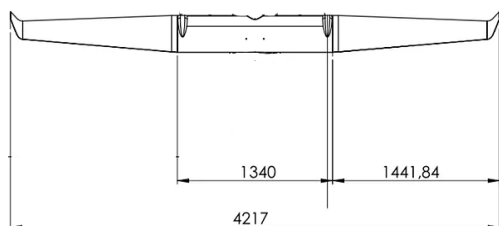


Figure 2 - External dimensions of the wing (mm) [5]

To accomplish the objectives, a structural linear elastic analysis of the UAV wing and its 3D model (half of the wing) was done using the *ANSYS Mechanical APDL* software. Related to the boundary conditions assumed, the *XFLR5* software was used to find the distributed lifting forces to apply on the wing. Besides that, a fixed end and a

symmetry boundary conditions were considered in the half wing tip that connects to the fuselage. The topology optimization was ensured by the “direct multisearch” solver (DMS). A derivative free method that executes a local search around a poll centre and uses the concept of Pareto dominance to define a list of nondominated points, from which the new iterates are chosen. The optimization design variables were defined based on the material thickness, quantity of carbon-epoxy laminas applied and on its carbon fibre orientations ($0^\circ/90^\circ$ or $\pm 45^\circ$). The *ANSYS* model was incorporated in the DMS solver.

2. ANSYS Mechanical APDL model

The topology optimization required the elaboration of a parametrized wing model. It was the most efficient approach, in terms of the engineering needs and goals, to simulate and optimize the structure of the UAV wing. As a consequence of that, was chosen the software *ANSYS*, namely the *Mechanical APDL* interface. A “bottom-up” strategy based programming was built from scratch to achieve the 3D wing model.

Since the wing is symmetric, it was modelled just half. A few geometrical approximations were done, due to time restrictions, namely the connection with the tail boom. Also the real wing is divided in two (for an easier transportation of the UAV), while the approximated model (*ANSYS* model) is a “one-piece wing”.

Was defined a structural linear elastic analysis, using the “SHELL181” element (4 nodes, 6 DoF per node). To define the wing geometry was created the key points, based on the wing airfoil. Those key points were united with lines and the gaps delimited by the lines were fulfilled, forming areas. Summing and subtracting areas, the internal holes (for the electrical cables) were made. At this point, the internal reinforcements and the exterior shape of the wing were modelled. Then, the mesh was created. Through the key points, the lines associated were identified and measured. Having that information, the lines were divided according to their size to maintain always the same number of divisions per section of line. By this way, even with the interior reinforcements and holes moving, the standardization of the mesh was ensured. As a consequence of that strategy, the mesh adapts to the moving parts of the wing.

Were considered and defined the materials used by the company: Carbon-epoxy composite (exterior skin, spars and

ribs) [7]; “Aluminium 6082 T6” (one rib) [8]; “Airex C70.75” (as the core material in: Spars, ribs) [9]. In order to verify the young’s modulus values of the carbon-epoxy composite material used in the wing, were done tensile tests in “Técnico Lisboa”. Considering that the carbon-epoxy composite specimens showed a brittle behaviour, and having the tensile stresses and strain values, the young’s model values were easily calculated using:

$$E = \frac{\sigma}{\epsilon} \quad (1)$$

The Table 1 summarizes the results from those tests.

Table 1 - Tensile tests results

Specimen	E_i [GPa]	$E_{average}$ [GPa]
1 (0°/90°)	65.3	62.46
2 (0°/90°)	62.3	
3 (0°/90°)	59.8	
4 (±45°)	12.7	12.63
5 (±45°)	12.6	
6 (±45°)	12.6	

Regarding the boundary conditions, was used the *XFLR5* software to simulate the loads that the wing must bear during stationary flight conditions. A 3D wing was modelled using that software and an aerodynamic analysis was done. The obtained distributed loads profile was applied on the key points of the ribs along the wing, in the *ANSYS* model (Figure 3). Besides that, since it was modelled half of the wing, in the tip opposing the winglet was applied a fixed end boundary condition (in the aluminium rib), simulating the carbon tubes used in the real wing. Finally, a symmetry boundary condition was applied on the same tip, but on the key points of the “exterior skin”, since the wing is symmetric.

In Figure 4 is showed the exterior shape of the wing (*ANSYS* model), while in Figure 5 are exhibited the internal reinforcements (*ANSYS* model).

The output values from the *ANSYS* model are written in a “output.txt” file. When the wing geometry is valid appears two values (maximum deflection (m) of the wing and its mass (kg)), when it is not, appears ∞ in both, instead (read the “Optimization” section, Equation 7). The maximum deflection of the wing corresponds to the value measured in the node located in the winglet tip. The mass value is calculated by

the *ANSYS* model, using the function “*GET” selecting all the elements of the wing.

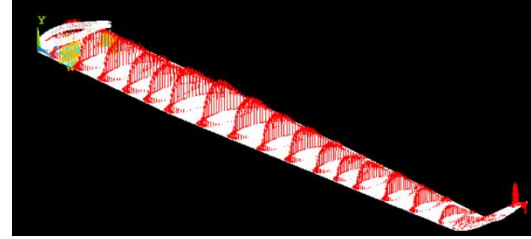


Figure 3 - Distributed lifting loads (*ANSYS* model)

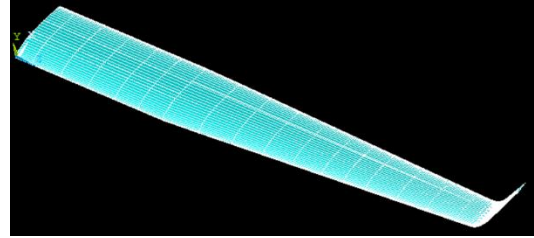


Figure 4 - Wing (*ANSYS* model)

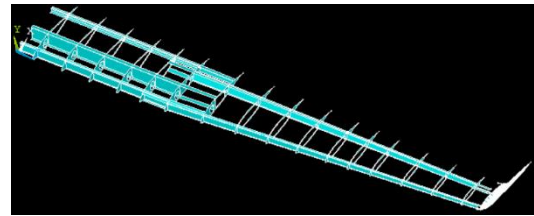


Figure 5 - Wing reinforcements (*ANSYS* model)

3. Optimization

A multiobjective problem can be defined as a practical application “where the designer may want to optimize two or more objective functions simultaneously” [10].

$$\mathbf{x} = (x_1, x_2, \dots, x_n)^T \in \Omega \subseteq \mathbb{R}^n \quad (2)$$

$$\min_{\mathbf{x} \in \Omega} F(\mathbf{x}) = (f_1(\mathbf{x}), f_2(\mathbf{x}), \dots, f_k(\mathbf{x}))^T \quad (3)$$

$$f: \Omega \subseteq \mathbb{R}^n \rightarrow \mathbb{R} \cup \{+\infty\} \quad (4)$$

Subject to:

$$h_i(\mathbf{x}) = 0; i = 1 \text{ to } p \quad (5)$$

$$g_j(\mathbf{x}) \leq 0; j = 1 \text{ to } m \quad (6)$$

where k is the number of objective functions, p is the number of equality constraints and m is the number of inequality constraints. \mathbf{x} is a n -dimensional design variables vector, $F(\mathbf{x})$ is a k -dimensional vector of objective functions and Ω the feasible region (the admissible set for the design variables). Note that maximize f_k is the same as minimize $-f_k$.

The authors in [6] presented a new multiobjective derivative-free methodology, the “direct multisearch” (DMS), which does not aggregate any of the objective functions. This method is based on a search step and a poll step. It uses the Pareto dominance concept, maintaining a list of feasible points (the best approximation to the Pareto front), nondominated points, from where the new poll centres are chosen. In every iteration, new nondominated points are added to this list, while the dominated ones are removed. When this list of feasible points changes, the iteration is considered as successful. When it doesn't, the iteration is considered as unsuccessful. The purpose of this method is to create the biggest amount of points in the Pareto front as possible, from the polling procedure. The local search step occurs around a poll centre, testing different directions scaled by a step size parameter. When an iteration is considered as successful, the step size parameter is maintained or increased, while in unsuccessful iterations it is decreased [6, 11].

Being the feasible region represented by Ω , it is used the follow barrier approach:

$$f_{\Omega}(\mathbf{x}) = \begin{cases} f(\mathbf{x}) & \text{if } \mathbf{x} \in \Omega \\ (+\infty, \dots, +\infty)^T & \text{otherwise} \end{cases} \quad (7)$$

Which means that the components of the objective function of an infeasible point is not

evaluated, allowing to deal with black box-type constraints [6].

There are different ways to generate the initial list of points (DMS variants), explained in the “chapter 6” of [11]. In the present work was used the “DMS (n, rand)”.

For a complete interpretation of the DMS solver is recommendable to read [6, 11].

The optimization process, using the DMS solver, is implemented using *MATLAB*. Was needed to code and edit some scripts to ensure the interaction with the *ANSYS Mechanical APDL* model. The goal is to find the nondominated points that minimize the two objective functions at the same time, which are: The maximum deflection value of the wing ($f_1(\mathbf{x})$) and its mass value ($f_2(\mathbf{x})$). The mass value represents the principal objective function to be optimized. The maximum deflection value, due to some of the geometrical approximations done, is expected to be lower than the one from the real wing. It is possible to formulate the problem in the following way:

$$\min_{\mathbf{x} \in \Omega} F(\mathbf{x}) = (f_1(\mathbf{x}), f_2(\mathbf{x}))^T \quad (8)$$

Subjected to:

$$\mathbf{x} = [x_1, \dots, x_{24}]^T \in \Omega \subseteq IR^n \quad (9)$$

Where the design variables are listed and described in Table 2.

Table 2 -Optimization design variables x_i

x_i	Value	Variable description
x_1	{10, 15, 20, 25, 30}	x position % of the spar 1
x_2	{35, 40, 45}	x position % of the spar 2
x_3	{65, 70, 75, 80}	x position % of the spar 3
x_4	{7, 14, 21, 28, 35, 42}	x position % of the spar 4
x_5	{2, 3, 4, 5}	No. of laminas, exterior skin
x_6	{1, 2}*	Carbon fibres orientation, exterior skin
$x_7, x_{10}, x_{13}, x_{16}, x_{19}$	{2, 3, 4, 5}	No. of laminas, spar $i = 1$ to 5
$x_8, x_{11}, x_{14}, x_{17}, x_{20}$	{0, 4, 8, 12, 16}	Core thickness, spar $i = 1$ to 5 (mm)
$x_9, x_{12}, x_{15}, x_{18}, x_{21}$	{1, 2}*	Carbon fibres orientation, spar $i = 1$ to 5
x_{22}	{2, 3, 4, 5}	No. of laminas, rib $i = 2$ to 16
x_{23}	{0, 4, 8, 12, 16}	Core thickness, rib $i = 2$ to 16 (mm)
x_{24}	{1, 2}*	Carbon fibres orientation, rib $i = 2$ to 16

In Table 2, the $\{1,2\}^*$ means: $1 \rightarrow 0^\circ \setminus 90^\circ$ or $2 \rightarrow \pm 45^\circ$. The first four design variables (x_1 to x_4) corresponds to the “ x position %” of the four mobile wing spars. It is measured from the leading edge of the wing, 0%, to the trailing edge, 100% (Figure 6 and Figure 7). The variables x_5 and x_6 correspond to the materials characteristics (no. of carbon-epoxy laminas and its carbon fibres orientation) of the exterior wing skin. The variables x_7 to x_{21} , are the materials characteristics of the five wing spars (no. of carbon-epoxy laminas, the thickness (mm) of the core material (“Airex C70.75”) and the orientation of the carbon fibres). The variables x_{22} , x_{23} and x_{24} are the material characteristics of the fifteen wing ribs (no. of carbon-epoxy laminas, thickness (mm) of the core material (“Airex C70.75”) and orientation of the carbon fibres).

The rib 1 is constituted by “Aluminium 6082 T6”, with a fixed 10 mm thickness and the spar 5 is fixed (x position). Because of that, those parameters are not design variables. Was considered a symmetrical lay-up, which means that the real number of the laminas is twice the values of the design variable.

Several optimization variables were defined due to the material variations in the UAV wing structure. The materials influence

directly the maximum deflection and mass values of the wing. The wing is mostly composed of carbon-epoxy composite and “Airex C70.75”. The “Aluminium 6082 T6” is used in one rib (rib 1), where the fixed end boundary condition is applied.

Associated to the composite material, there are two parameters: The orientation of the fibres ($1 \rightarrow 0^\circ \setminus 90^\circ$ or $2 \rightarrow \pm 45^\circ$) and the number of laminas (0.2 mm of thickness each). Related to the core material foam (“Airex C70.75”), there is only one parameter: Its thickness (mm). In the optimization process was considered its use (thickness $\neq 0 mm$) or not (thickness = 0 mm).

Considering that the external skin is made by carbon-epoxy laminas and each spar (total no. = 5) and rib (total no. = 15) by carbon-epoxy laminas and “Airex C70.75” (as the core material, if its thickness is different from zero), Table 2 resumes the design variables values. Note that of the fifteen ribs only result three parameters, having all the same material characteristics.

Therefore, there are 24 design variables: 4 (x position of the spars), 2 (material of the exterior skin), 15 (materials of the spars), 3 (materials of the ribs).

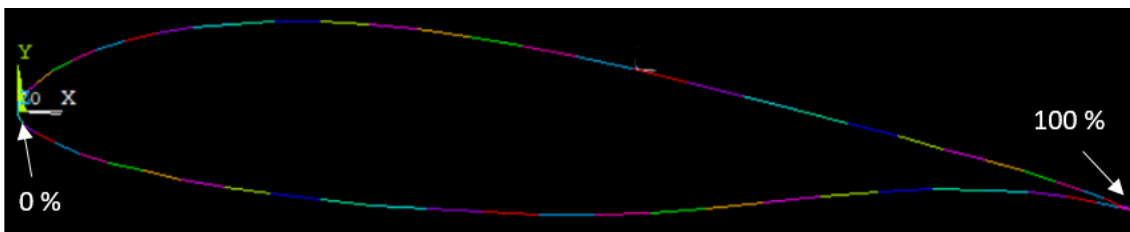


Figure 6 - Wing airfoil, front view (ANSYS model)

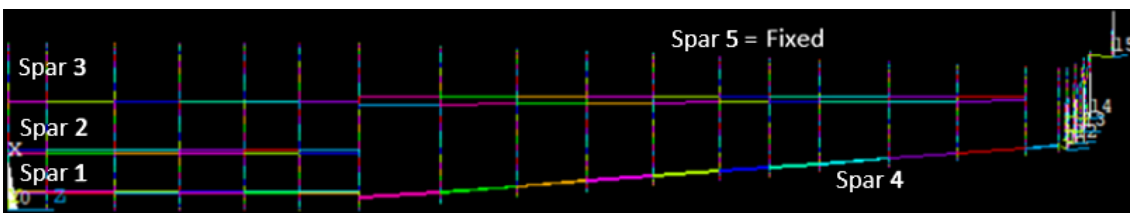


Figure 7 - Structural reinforcement components (ANSYS model)

4. Results

In Table 3 are some of the optimization design variables values referring to the wing currently used. The (total) wing is weighing 5 kg and the only maximum deflection value measured is the one from a wing test done by the company (200 mm), where the wing

geometry tested corresponded to an incomplete and more fragile structure. That value is not in the order of magnitude expected, due to all the simplifications and missing structural components of that wing tested.

Comparing to the wing model from ANSYS, the values of the maximum

deflection from the real wing, should be higher. In the numerical model it was modelled a “one-piece wing”, while the real one is divided in two.

Related to the weight of the wing, the values obtained from the simulation are expected to be in the same order of magnitude.

Table 3 - Current wing geometry design values

Detail	Value
Mass	<i>total wing: 5 kg</i>
<i>X</i> position of spar 1	34 %
<i>X</i> position of spar 2	58 %
<i>X</i> position of spar 3	82 %
<i>X</i> position of spar 4	32 %
Carbon fibre Orient.	$\pm 45^\circ$ and $0^\circ/90^\circ$
“Airex C70.75” max thickness	12 mm

Another relevant comparison between the wing currently used and the ANSYS model, is the rib made by aluminium, once it is the densest material in the wing constitution. In the ANSYS model it was approximated to a simpler geometry (more material). At first sight, it is intuitive to think that by this way it will increase considerably the weight results from the optimization process. Whereas, the fact is that the ANSYS model does not consider the weight of the electrical cables and some pieces needed to the ailerons and flaps. As a consequence of that, the weight results from the optimization process are balanced.

Adapting the design variables known from the wing geometry being used (Table 3) to the ANSYS model (half wing), were obtained the following objective functions values (Table 4).

Table 4 - Current wing geometry (ANSYS model)

Objective Function	Value
Maximum deflection	$\approx 0.0375 m$
Mass	2.5 kg

From Table 4, can be seen that the mass value is the same as the real wing being used (half wing = 2.5 kg \Rightarrow complete wing = 5kg). This simulation confirms the feasibility

of the ANSYS model. From now on, the objective functions values obtained (Table 4) from the ANSYS model of the wing geometry currently used are the limit ones (remember that both objective functions should be minimized).

Knowing that the complete wing currently used weights 5 kg (Table 4) and that the results from the optimization process refer to half of the wing, the maximum value of weight acceptable from the optimization results must be under 2.5 kg (red line in Figure 8). Due to that fact, three of the four regions of nondominated points have to be discarded, the ones above the red line in Figure 8. This restriction was not considered during the programming phase because the “UAVision” wanted all the possible solutions, once depending on the mission, are implemented more or less instruments (e.g. cameras) on the wing, being its maximum deflection and mass values variable. At this point, considering just the mass limitation, there are no constraints in terms of the maximum deflection value, since it was proved that a more fragile and incomplete structure withstands considerably larger deflection values than the ones obtained from the optimization process. Because of that, is possible to limit the range of possible values acceptable for this problem based on the points affected by the weight constraint.

From the 358 possible solutions there are now 81 solutions acceptable for the problem, delimited by the red and green lines in Figure 8.

Considering now the simulation results of the maximum deflection from the Table 4, of the 81 possible solutions are considered 17 as acceptable (Figure 9). In Figure 9 are marked (red and blue lines) the current wing geometry objective function values (from the ANSYS simulation (Table 4)), delimiting those 17 acceptable solutions (point A to point C). This decrease on the number of solutions happens once is expected to minimize both objective functions, with greater importance to the wing mass.

Of those 17 acceptable solutions, were chosen 3 to be analysed: Point A, point B and point C. Point A and point B once they are the two “end points” of the 17 acceptable solutions, i.e., point A has the highest minimized maximum deflection value ($\approx 0.0375 m$) and the lowest minimized mass value (2.3 kg), while the point C has the opposite, minimized maximum deflection value of $\approx 0.0374 m$ and minimized mass value of 2.49 kg. The point B is the one with its objective functions values (min(mass):

2.37 kg; min(maximum deflection): ≈ 0.0374 m) between the other two (with both objective functions values lower than the current wing objective functions values). The x position of the spars of the wing geometries correspondently to those points are evidenced in Table 5.

Table 5 - X position of the spars (point A, B and C)

Description	Point A	Point B	Point C
Spar 1:	30 %	30 %	30 %
Spar 2:	40 %	40 %	40 %
Spar 3:	65 %	65 %	65 %
Spar 4:	35 %	35 %	35 %

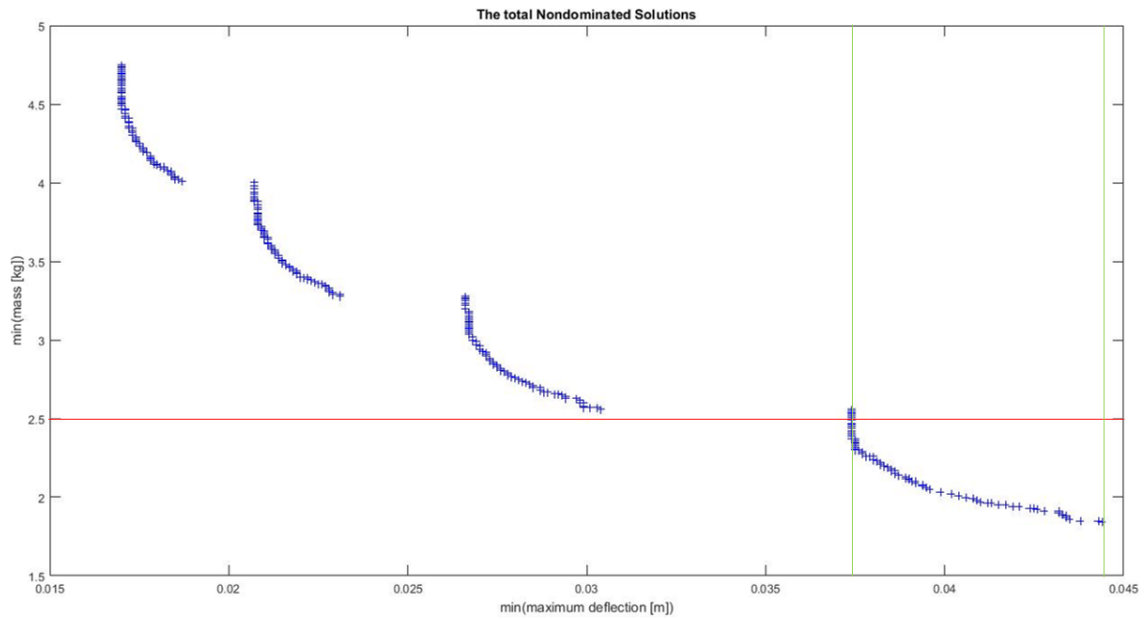


Figure 8 - All the possible solutions

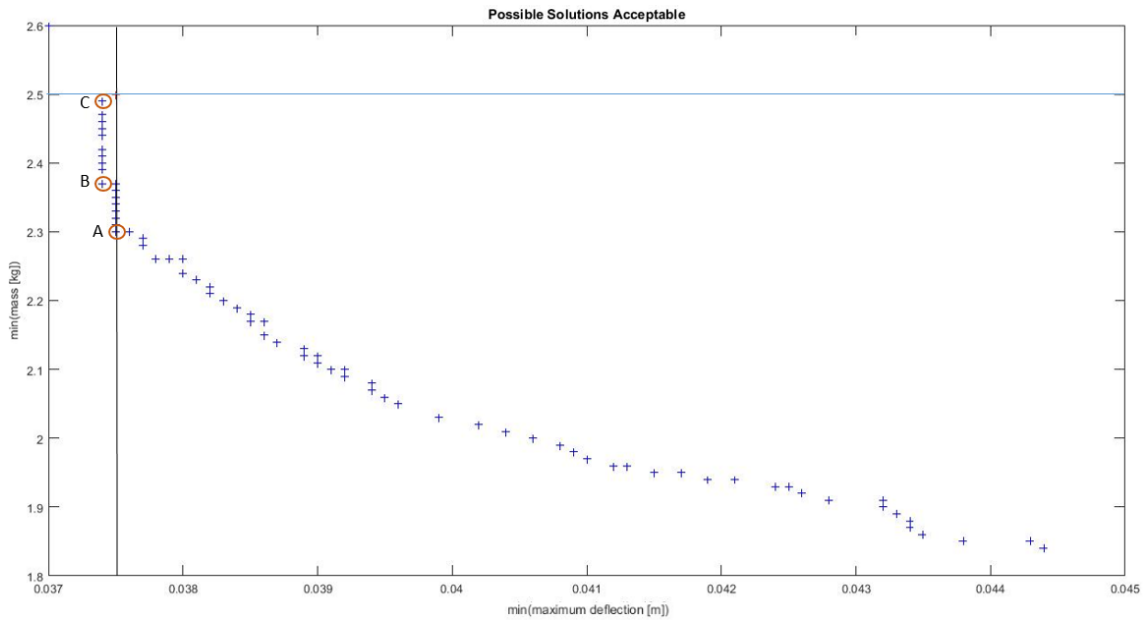


Figure 9 - The acceptable solutions

Related to the minimized mass values (half wing), point A has the minimum value, while the point C has the maximum (difference of 0.19 kg between those two acceptable solutions). Their minimized maximum deflection values are similar. The x position of the spars is the same for those three geometries. Comparing it to the ones from the currently wing being used (Table 3), is noticed that the x position values of the spars 2 and 3 are the ones with a bigger difference. While in the current wing geometry the spars are more distributed and close to the trailing edge of the UAV wing (32 % to 80 %), in the optimized ones they are located more in the centre region of the wing (30% to 65%). By this way the spars are higher (higher inertial \Rightarrow lower stress), reducing the number of laminas used (\Rightarrow lower mass value). Comparing the number of carbon-epoxy laminas and the orientation of the carbon fibres in the structural components, there are no considerable differences.

It is prioritised the minimization of the mass. Of the 17 acceptable solutions, the point A corresponds to the optimal wing geometry from the optimization process. Besides having an approximated maximum deflection value ($\approx 0.0375 m$) to the one from the current wing geometry, its mass minimization corresponds to a decrease of 8%. Based on that, is expected to have a "complete" wing weighting 4.6 kg, instead of the prior 5 kg. Related to the minimization of the maximum deflection wing value, the maximum decrease achieved is with the point C ($\approx 0.0374 m \rightarrow 0.3\%$ decrease). Those remarks are summarized in Table 14.

Table 6 - Optimization remarks

Objective Function	Description (complete wing)
min(maximum deflection)	max decrease of 0.3 %
min(mass)	max decrease of 0.4 kg (8%)

To validate those three solutions (Point A, B and C), generalizing its analysis results to the other 14 acceptable solutions, was done a structural analysis using the ANSYS model. Knowing from the tensile tests done that the ultimate tensile stress value of the "epoxy + bi carbon fibre +45°/-45°" is 100 MPa and considering that the "epoxy + bi carbon fibre 0°/90°" showed a better mechanical behaviour, that value was considered as the critical one.

From the ANSYS model, in the spar 5 of (wing geometry) point A (constituted by "epoxy + bi carbon fibre +45°/-45°"), the maximum value of tensile stress verified was 5.46 MPa ($< 100 MPa$). For the spar 5 (constituted by "epoxy + bi carbon fibre +45°/-45°") of the point B (wing geometry), the maximum tensile stress value verified was 5.21 MPa ($< 100 MPa$). By this way, was validated the structural behaviour of the "epoxy + bi carbon fibre +45°/-45°" based wing components.

Considering the entire wing, all those three geometries show their maximum tensile stress values in the skin ("epoxy + bi carbon fibre 0°/90°") of the wing, in the fixed end (boundary condition) zone. This result was expected and the tensile values (A – 86.9 MPa ; B – 86.2 MPa; C – 86.5 MPa) are still lower than 100 MPa. Since from the tensile tests made there are no information for the ultimate tensile stress for the "epoxy + bi carbon fibre 0°/90°", but was verified that it bore higher loads, can be extrapolate the viability of the structure by this way.

The results obtained with the point A, point B and point C were generalized for the other 14 acceptable solutions. Between the 17 acceptable solutions, the design variables values don't have a considerable variation, being reasonable this approach.

From now on, is expected the manufacture and test of the point A (the optimal wing geometry obtained), in order to validate it experimentally (it was not possible to be done during this work, due to the unavailability of "UAVision").

5. Conclusions

The present work was an opportunity to work directly with a company, the "UAVision". By this way was possible to deal with a real need of the company, working in an engineering environment, namely in a place where the design and the manufacture of their products is done. The fact of being with the engineers and the workers in the production area, make possible to understand and experience the routines and dynamics of the company.

This work was presented by me in the "6th International Conference on Engineering Optimization", that took place in "Técnico Lisboa", between the 17th and 19th of September of 2018.

Related to the 3D modelling phase, using the ANSYS software (*Mechanical APDL* interface), several geometrical approximations were done, in order to

simplify the problem due to restrictions of time. Those simplifications affected the maximum deflection values (model: "one-piece wing"; real wing: divided in two). Besides that, the values obtained from the optimization process were acceptable. Not having a previous test made with the current wing geometry (in the structural point of view), resulted in a lack of information for comparison with the values from the model. Related to the mass values obtained, and comparing it with the ones known from the real wing, they were in the same scale of values. Based on the similarities with the real wing, in terms of the materials used and the structural components of the wing, the mass results were expected to be quite satisfactory. Note that were considered stationary flight conditions for the distributed forces applied on the wing.

In the optimization process was used the DMS solver. Were considered 24 design variables taking into account the materials of the structural components and the x position of the spars. The discrete values were chosen considering the thickness of the wing components and the wing geometry possibilities. For this stage was used the *MATLAB* software (inside the DMS solver, the *ANSYS* model was executed). Were obtained several wing geometries, with different values of maximum deflection and mass. The results proved once again that this solver can be used in practical examples and that it is functional. Were considered as acceptable solutions 17 wing geometries (from the initial 358), from which the optimal one corresponds to a reduction of 0.4 kg of mass (complete wing), while the maximum deflection value maintained approximately the same as the one from the current wing geometry (from the *ANSYS* model result ($\approx 0.0375 m$)). In this type of structures, maintaining the structural components and the materials, this reduction of weight is considerable and improves the performance of the vehicle. In terms of the maximum deflection value, there was no big reduction (0.3%). However, since there was not enough information (maximum deflection) about the current wing geometry, there are no further conclusions besides the ones already mentioned.

Related to the carbon fibre orientation, the "epoxy + bi carbon fibre 0°/90°" was the preferred. Based on its higher young's modulus and its mechanical behaviour (better than the "epoxy + bi carbon fibre +45°/-45°"), this result was expected.

Based on the optimized wing geometries analysed (point A, B, C) was verified that the spars were tendentiously located more to the centre of the wing (x position), when compared to the geometry currently used. In fact, that location make them (the spars) higher, increasing their inertia momentum and as a consequence decreasing the stresses. By this way is possible to reduce the number of carbo-epoxy laminas in their constitution and as a consequence cause a decrease in the weight of the wing. Note that the spars are subjected mainly to bending. These solutions were verified based on the tensile stress analysis, using the *ANSYS* model. That verification was generalised for the other 14 acceptable solutions, since there were not verified considerable differences between those wing geometries.

Based on the work done and the results obtained, the objectives were accomplished, namely in terms of the mass reduction. The DMS solver was applied correctly and the 3D wing model (*ANSYS*) programmed corresponds to a viable wing approximation.

6. References

- [1] Bone, E., Bolkcom, C. (2003). Unmanned Aerial Vehicles: Background and Issues for Congress Current. Report for congress, Congressional Research Service. The Library of Congress
- [2] Sullivan, J. M. (2006). Evolution or revolution? The rise of UAVs. *IEEE Technol. Soc. Mag*, vol. 25, pp. 43 - 49
- [3] Pereira, E., Bencatel, R., Correia, J., Félix, L., Gonçalves, G., Morgado, J., Sousa, J. (2009). Unmanned Air Vehicles for Coastal and Environmental Research. *Journal of Coastal Research. Proceedings of the 10th International Coastal Symposium ICS 2009*, vol. 2, pp. 1557-1661
- [4] Nomani, K. (2007). Prospect and Recent Research & Development for Civil Use Autonomous Unmanned Aircraft as UAV and MAV. *Journal of System Design and Dynamics*, vol. 1, pp.120-128
- [5] UAVision. (2018). Website of UAVision Company, <https://www.uavision.com/>, accessed at the 6th of July.
- [6] Custódio, A. L., Madeira, J. F. A., Vaz, A. I., F., Vicente, L. N. (2011). Direct Multisearch for Multiobjective Optimization. *SIAM J.Optim.*, vol. 21, pp. 1109-1140

[7] Performance composites. (2018). Website of Performance Composites Ltd., http://www.performance-composites.com/carbonfibre/mechanicalproperties_2., accessed at the 12th of March.

[8] Core Materials. (2018). Website of Airex AG., <http://www.airexag.ch/de/startseite.html>., accessed at the 12th of March.

[9] Aluminium Alloy. (2018). Website of Aalco Metals Ltd., http://www.aalco.co.uk/datasheets/Aluminium-Alloy_6082-T6~T651_148.ashx., accessed at 12th of March.

[10] Arora, J. (2011). Introduction to Optimum Design (3rd ed.). Academic Press. Chapter 17. ISBN 9780123813763

[11] Custódio, A. L., Emmerich, M., Madeira, J. F. A. (2012). Recent Developments in Derivative-free Multiobjective Optimization. Computational Technology Reviews, vol. 5, pp. 1-30